The Study of the Correlation between the Detection Limit and the Energy Stability of Two Antimony Complexes by Means of Conceptual DFT

Naceur Benhadria[1, 2], Boulanouar Messaoudi[1, 3] and Tarik Attar[1, 4, *

[1]École supérieure en sciences appliquées P.O. Box 165 RP, Tlemcen, 13000, Algérie
[2]Laboratoire de chimie des matériaux inorganiques et application, Université des Sciences et Technologie d'Oran Mohammed Boudiaf (USTO M.B). PB 1505 El M'naouar 31000 Oran, Algérie.
[3]Laboratoire de Thermodynamique Appliquée et Modélisation Moléculaire, Département de Chimie, Faculté des Sciences, Université A. Belkaid, BP 119, Tlemcen, 13000, Algérie.
[4]Laboratoire de Toxicomed, Université Abou Baker Belkaid, BP119, 13000 Tlemcen, Algérie.
*Corresponding author: (e-mail: t_attar@mail.univ-tlemcen.dz)

Two organometallic complexes, catechol-antimony and pyrogallo-antimony were theoretically studied by means of density functional theory (DFT) calculations. The concept of detection limit in electroanalysis was put in evidence by quantum chemical calculations onto antimony trace analysis in aqueous solution by using pyrogallol (1, 2, 3-trihydroxybenzene) and catechol (1,2-dihydroxybenzene) as ligands. Based on two previously published works, the study was carried out experimentally by polarography technique where the working electrode was a dropping mercury electrode. The DFT study, carried out at the 6-31G* and 3-21G* basis sets combined to LSDA/B3LYP method, showed the existence of a very strong relationship between the total energy of antimony complexes and the detection limit; thus the more stable complex has the better detection limit value. Based on the Fukui indices, the calculated parameters such as local nucleophilicity indices and HOMO-1 electronic density of the ligands showed a high interaction of antimony(III) with pyrogallol than that with catechol. This finding was in good agreement with the experimental results.

Key words: Antimony complexes; selectivity; Fukui indices; DFT calculations

Antimony is of a significant environmental concern because of its high toxicity depending on the chemical species and oxidation state. Antimony exists mainly in the pentavalent Sb(V) and trivalent Sb(III) oxidation states in most natural systems. Sb(III) compounds are more toxic than Sb(V) compounds by a factor of 10. The contamination caused by this kind of pollutant comes from water or fruit juices bottled commercially in plastics because antimony trioxide which is used in the polymer industry as a polycondensation catalyst for polyethylene terephthalate production [1]. Two reviews dealing with the properties and the environmental chemistry of antimony were published by Filella *et al.* [2, 3]. The use of electrochemical techniques is of considerable importance in analytical techniques due to their high degree of sensitivity, accuracy, precision, and selectivity as well as large linear dynamic range, with relatively low-cost instrumentation [4-6]. Its various applications cover many fields going from environment, metal industry, pharmaceutical, and clinical to food and industrial samples. Among the electrochemical methods used for the determination of trace element species, the adsorptive stripping voltammetry (AdSV) is considered as a powerful technique because of its wide linear dynamic range and low detection limit w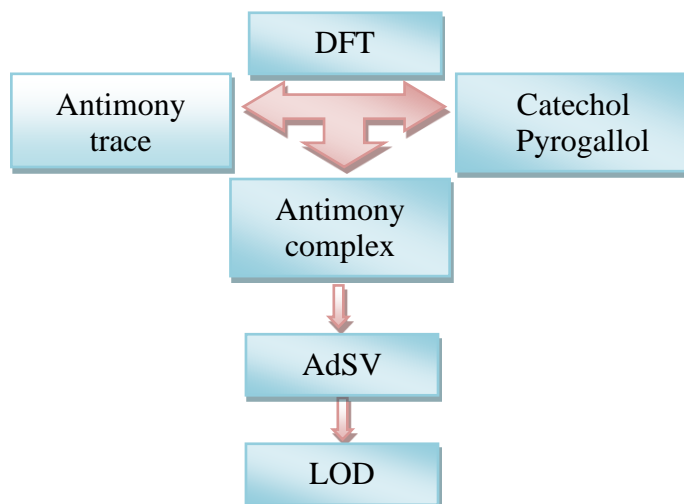hich is achieved as the result of performing the preconcentration steps directly into the voltammetric cell [7]. The AdSV method is capable to analyze metallic ions with concentration up to ppb level [8-10]. Thus, adsorptive stripping analysis becomes a widely accepted tool to determine trace amounts like antimony ions [11, 12]. In this method, metal ions with adequate surface-active ligands are converted into stable complexes. Prior to the voltammetric scan, the formed complexes are adsorbed onto the working electrode by means of a non-electrolytic process [13, 14]. The AdSV method is relatively inexpensive, small in size, requires low levels of electrical power, and is sufficiently portable to permit its use in the field [15]. It also has a convenient possibility to analyze various samples without the need of a prior separation. Adsorptive preconcentration of Sb(III) can be achieved using different organic ligands such as catechol and pyrogallol, allowing antimony determination with the best limit of detection (1.3×10^{-9} M for catechol and 1.03×10^{-10} M for pyrogallol) [16, 17]. In principle, when a ligand is bound to a metal ion, a metal-ligand complex is formed, resulting in a great change in the global energy between the ligand and complex.

The catechol molecule got attention and was also studied theoretically. Many of the researches

112 Naceur Benhadria, Boulanouar Messaoudi and Tarik Attar

The Study of the Correlation between the Detection Limit and the Energy Stability of Two Antimony Complexes by Means of Conceptual DFT

were focused on finding the kinetics and mechanism of catechol decomposition, oxidation, and implication in various domains such as in biology when dealing with enzymes and its oxidative activity [18-21]. For instance, Mohammednoor et al. probed the reaction pathways for the unimolecular decomposition of catechol and its kinetics [22]. Zhang et al. employed B3LYP DFT method in conjunction with 6-31G(d,p) basis set to reveal the substituent effects on O-H bond dissociation enthalpies and ionization potentials of catechol derivatives. They proved that 1,4-pyrone was unlikely to be favorable to enhance the H-abstraction activity of flavonoids [23]. Moreover, other theoretical studies dealt with geometrical and electronic properties of catechol. Vedernikova et al. did a DFT investigation, using different basis sets, on catechol and its conformers. Basically, they calculated the geometry, electronic structure, and local charge fluctuations in catechol. They paid more attention to the effect of the hyperconjugation and used hardness indices to describe the interrelationship between internal hydrogen bonding and stabilization of neutral or charged radicals. They found the effect of hyperconjugation on the strong delocalization of the responsible σ orbital and the strong localization of the related π orbital [24]. Walther et al. studied the molecular structure of catechol by microwave spectroscopy combined with ab initio geometry refinements of two different basis sets, 4-21G, and 4-21G*. They showed that the experimental rotational constants of catechol can be reproduced by a geometry in which the C-O bond lengths are 1.409 and 1.395 Å [25]. More papers on chelated geometry of catechol could be found in the literature such as the chelation on TiO_2 [26]. On the other hand, pyrogallol got too much attention too in various theoretical studies. Vedernikova et al. used the Kohn–Sham LCGTO-DFT program deMon-KS to investigate the conformational behavior of pyrogallol. They found three characteristic structures on the potential energy surface of the compound: the Anti form, in which the hydrogen points away from the hydroxyl groups, and the two Syn forms (the hydrogen points towards the hydroxyl groups). They performed a DFT-based theoretical analysis of hyperconjugation and orbital delocalization effects using hardness indices in order to study the subtle mutual influence of hyperconjugation and hydrogen bonding in pyrogallol compounds [27]. Riahi et al. calculated the oxidation potentials of pyrogallol and some of its derivatives in aqueous solutions using ab initio molecular orbital calculations, and density functional theory (DFT). In order to describe the solvent effect, they applied polarizable continuum model. The obtained experimental results with the aid of an electrochemical technique (cyclic voltammetry) were found to be in good agreement with the theoretical oxidation potential values of the studied pyrogallol and its derivatives [28]. Ji et al. studied and calculated four homolytic O–H bond dissociation enthalpy (BDE) of pyrogallol by means of a coupled-cluster method with single and double excitations (CCSD) at the 6-31+G* level. While one of these calculations supported the experimental value determined by time-resolved photoacoustic calorimetry, the three remaining BDE were reported for the first time and would provide deeper insights into the H-atom donation behavior of pyrogallol [29]. Add to this, the highest hydroxyl radical scavenging efficiency and pyrogallol autoxidation inhibition efficiency have been found, both experimentally and theoretically, to be important in developing antioxidants with high efficiency that are fundamental for the protection of living cells and engineering materials against oxidative damage [30-33].

In the present study we used the DFT method to provide a relevant insight into molecular electronic properties of organometallic complexes, their formation, and stability. To the best of our knowledge, there is a lack of theoretical data about the metal trace in terms of detection limit relationship to complex formation energy and there is no scientific report on the DFT study of this feature dealing with polarography technique. The concept of the detection limit has been defined as an analyte concentration that yields a signal in the measurement instrument (y) which is significantly different from that obtained for the blank [34, 35]. Hence, based on the experimental results [16, 17], our study was subdivided as follows. Firstly, we have analyzed whether the experimental results were obtained under the same conditions in the AdSV technique. Among the parameters widely controlled in this technique, we can cite potential and time of adsorption. Secondly, we have conducted a DFT calculus of ligands, metal, and formed complexes. At the end, the LOD values given by the AdSV technique for each metal would be correlated with the results of the DFT study. A research methodology flowchart is given to clarify the steps that were followed in this study (Scheme 1). The novelty of this theoretical study was to shed light on DFT calculations of two antimony complexes and their relationship in terms of energy of stability with the limit of detection for each complex. Therefore, the DFT method aimed to explore the geometrical, electronic structure, and thermodynamic parameters of catechol, pyrogallol, and their corresponding complexes. In addition, several molecular descriptors were calculated with the aim to explore some of their electronic properties and to point out the most probable reactive sites for electrophilic attack, in particular for metal coordination. For this reason, some quantum parameters like the energies of the frontier molecular orbitals, the band gap, electronegativity, chemical potential, global hardness, and global softness, that are very useful tools to understand the relationship between the best detection limit and complex formation stability energy, were investigated.

113 Naceur Benhadria, Boulanouar
Messaoudi and Tarik Attar

The Study of the Correlation between the Detection
Limit and the Energy Stability of Two Antimony
Complexes by Means of Conceptual DFT

Scheme 1. Flowchart of the study

COMPUTATIONAL METHODS

Computational Details

The calculations were carried out using the Density Functional Theory (DFT) with the LSDA method [36] and 6-31G(d) basis set, implemented in Gaussian 09 program package [37]. The geometry optimizations and frequency calculations at this level of theory were performed for all the stationary points. The finite difference approximation (FDA) was used to calculate the Fukui indices. We note that the geometry of the neutral system was kept for both cationic and anionic systems in the calculations of local indices. The electronic population calculations were carried out using both MK (Merz-Singh-Kollman) and NPA (natural population analysis) [38].

In density functional theory (DFT), the local spin density approximation (LSDA) is the most used approximation for the exchange-correlation energy $E_{xc}[\mathbf{n(r)}]$ [39]:

$$E_{xc}[n(r)] \approx E_{xc\,LSDA}[n(r)] = \int \epsilon_{xc}\,(n\uparrow(r),n\downarrow(r))n(r)d^3r \quad (1)$$

Where, ϵ_{xc} means the exchange-correlation energy per electron of the spin-polarized homogeneous electron gas which is a model system frequently used in electronic structure theory. The quantities $n^\uparrow$ and $n^\downarrow$ denote spin-up and spin-down densities. They are obtained by rotating the spin quantization axis at each point in space in the direction that yields a diagonal spin density matrix. E_{xc} depends upon electron density (ρ) at each point in space, i.e., local value of ρ. The LSDA method allows electrons with opposite spins to have different spatial Kohn-Sham orbitals.

Global Reactivity Indices

The electronegativity [40] (χ) and hardness (η) of a substance [41] have been provided with rigorous definitions within the purview of conceptual density functional theory (DFT) [42]. Electronegativity is defined as the negative of chemical potential and for an N-electron system with total energy E and external potential $v(r)$ [43]. This term is calculated by the following equation [44]:

$$\chi = -\mu = -\left(\frac{\partial E}{\partial N}\right)_{v(r)} \quad (2)$$

μ is the Lagrange multiplier associated with the normalization constraint of DFT [45]. Hardness (η) is given by the following relationship [46]:

$$\eta = \left(\frac{\partial^2 E}{\partial N}\right)_{v(r)} = \left(\frac{\partial \mu}{\partial N}\right)_{v(r)} \quad (3)$$

By using the finite difference method, χ and η can be also calculated as [47]:

$$\chi = \frac{I+A}{2} \quad (4)$$

$$\eta = I - A \quad (5)$$

Where A and I are the electron affinity and ionization potential, respectively. If ϵ_{HOMO} and ϵ_{LUMO} are the energies of the highest occupied and lowest unoccupied molecular orbitals, respectively, then the above equations can be rewritten, using Koopmans' theorem as [48]:

$$\chi = -\frac{\epsilon_{HOMO} + \epsilon_{LUMO}}{2} \quad (6)$$

$$\eta = \epsilon_{LUMO} - \epsilon_{HOMO} \quad (7)$$

The electrophilicity index is given by [49]:

114 Naceur Benhadria, Boulanouar
Messaoudi and Tarik Attar

The Study of the Correlation between the Detection
Limit and the Energy Stability of Two Antimony
Complexes by Means of Conceptual DFT

$$\omega = \frac{\mu^2}{2\eta} \qquad (8)$$

The electrophilic power of a system can be quantified by this equation. Basically, we cannot define the nucleophilicity index by variational procedure, due to the non-stabilization of molecular electronic structure along the subtraction of electron-density of a given molecule. In the case when a nucleophilic descriptor is absent in simple molecules, Domingo *et al.* [36] proposed that the lesser electrophilic is a molecule, the more nucleophilic it is. For complex molecules with several functional groups as the captodative ethylenes (CD), good nucleophiles and good electrophiles could be concurrently presented in the same molecule [50]. Recently, Domingo's group has proved that the nucleophilic character of a molecule can be related with the feasibility to remove electron-density. This simplest approach to nucleophilicity can be written as a function of negative value of the gas phase (intrinsic) ionization potentials (IPs) calculated within the framework of molecular orbital theory, namely,

$$N = - IP \qquad (9)$$

from which high (low) nucleophilicities become naturally associated to low (high) ionization potentials. Within this context, the intrinsic nucleophilicity (i.e., associated to the negative of the gas-phase IPs) is thereafter corrected by differential solvation energies of species [51]. The nucleophilicity (N) index can be defined as [52]:

$$N = \varepsilon_{HOMO(Nu)} - \varepsilon_{HOMO(TCE)} \qquad (10)$$

Where $\varepsilon_{HOMO(Nu)}$ and $\varepsilon_{HOMO(TCE)}$ are referred to the highest occupied molecular orbital (HOMO) energies obtained within the Kohn–Sham scheme for a molecule and tetracyanoethylene (TCE), respectively. Note that the TCE molecule is taken as a reference because it presents the lowest HOMO energy in a large series of molecules already investigated in the context of polar DA cycloadditions [53]. The feasibility of such N index describing the nucleophilic behavior of an organic molecule has been previously tested in the context of the analysis of the nucleophilic nature of captodative ethylenes (CD ethylenes) [50].

Local Reactivity Indices
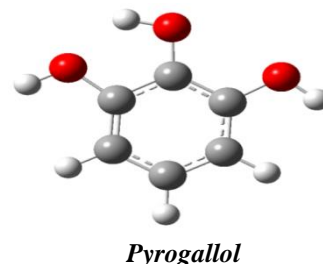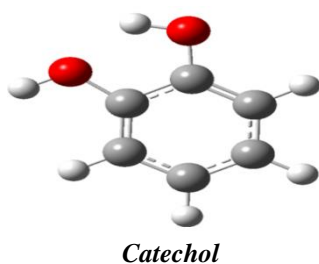
The reactivity/selectivity of a specific site in a molecule was quantified by the local quantities such as the Fukui function *f(r)*. The Fukui function at a constant external potential, *v(r)* is given by:

$$f(r) = \left[\frac{\partial \rho(r)}{\partial N} \right]_{v(r)} = \left[\frac{\delta \mu}{\delta v(r)} \right]_N \qquad (11)$$

Where $\rho(r)$ represents the electronic density of a system and N the number of electrons [54]. Several different methods have been proposed to approximate the derivative. The condensed form of the Fukui function introduced by Yang and Mortier [55] consists to assign one value f_k on each atom *k* of the molecule. They further used the finite difference approximation (FDA) yielding to the following definitions:
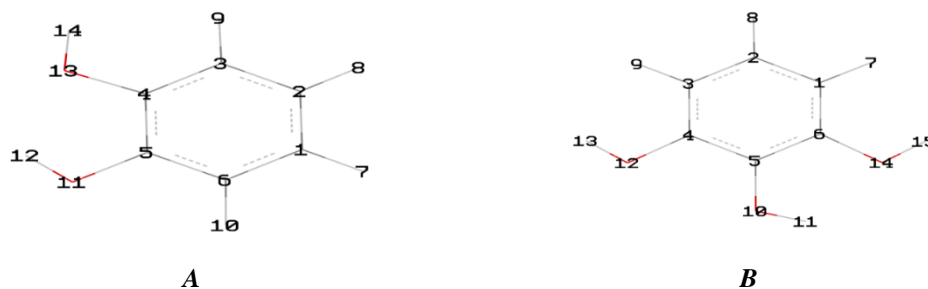for Nucleophilic attack

$$f_k^+ = \left[\rho_k(N+1) - \rho_k(N) \right] \qquad (12a)$$

for Electrophilic attack

$$f_k^- = \left[\rho_k(N) - \rho_k(N-1) \right] \qquad (12b)$$

where $\rho_k(N)$, $\rho_k(N-1)$ and $\rho_k(N+1)$ are the gross electronic populations of the site k in neutral, cationic, and anionic systems, respectively.

The Mulliken, natural, electrostatic population analysis can be used to calculate charges on each molecule. The two above equations (12a, b) have been applied to a variety of systems looking for reactivity trends [56, 57]. However, the main concern in using FDA approximation is that its accuracy depends on the type of population analysis used and that is critical for anionic systems. The molecular structures used in this study are shown in Figure 1. These substances can be used as ligands in the formation of complexes. The tendency to form a complex in this case was explained by the presence of high electronic density on the neighbouring oxygen atoms in each molecule. This heteroatom had an important effect on the adsorption phenomenon on the metal surface, in addition to their large molecular surface that induced a widespread covering of the surface of the metal. The goal of this study was to give a deeper insight of the ligand effect on the detection limit and its relationship to the stability of the studied compounds (Fig.1) by means of DFT-based reactivity indices.

Catechol   *Pyrogallol*

Figure 1. Molecular structures of catechol and pyrogallol.

115   Naceur Benhadria, Boulanouar
      Messaoudi and Tarik Attar

The Study of the Correlation between the Detection
Limit and the Energy Stability of Two Antimony
Complexes by Means of Conceptual DFT

Figure 2. Atoms labelling for catechol (*A*) and pyrogallol (*B*).

RESULTS AND DISCUSSION

The structures of molecules can affect the adsorption by influencing the electron density of the functional groups. In order to rationalize the local reactivity, we have calculated the Fukui indices, f_k using the labelling shown in Figure 2. The results are given in Tables 2 and 3. The Fukui indices, f_k^- corresponding to electrophilic attack were calculated using natural population analyses (NPA) to have a clear idea about the most reactive sites of the studied compounds.

The analysis of the local nucleophilicity indices given in Table 3 showed that oxygen atoms O11 and O13 and carbon atom C2 for catechol were characterized by the highest values of the local nucleophilicity indices. Although C2 had a higher N_k, it was very far from a complex formation with the antimony atom. For pyrogallol, oxygen atom O10 had the highest N_k value. O12 and O14 were characterized with lower N_k values with respect to C2 and C5. It was obvious that the latter could not go through complexation. O12 and O14 atoms had different values of the local nucleophilicity indices which were not realistic since the molecule was symmetrical, so O12 and O14 had to get similar N_k values.

As a result, the oxygen atoms of the two studied molecules were the most reactive centers, which involved a greater ability to bind to the metal surface. Consequently, the analysis based on the static DFT-based indices correctly predicted the regioselectivity of these complexes and was then in good accordance with experiment. On the other hand, the distribution of electron density of frontier molecular orbitals is of importance when dealing with such reactions. The HOMO provides a good proof and evidence on the reactivity of this region (Fig. 3). Density is important in the area containing the oxygen atoms. Its visualization showed a large distribution on the oxygen atoms and the neighbouring regions. Therefore, we could conclude that this area was the region of reactive centers that transfer electrons from oxygen atoms to the antimony surface. HOMO and LUMO energies, from Table 1, had been examined in order to find the tendency of each ligand to donate electrons (to empty molecular orbitals with low energy of convenient molecules), or to accept electrons, respectively. The resulting band gap ΔE (E_{HOMO} - E_{LUMO}) could be used to provide useful information on the chemical reactivity and kinetic stability of each ligand [58, 59]. The band gap calculated for the HOMO and LUMO energies (Table 1) of pyrogallol was higher than that of catechol. Thus, according to the obtained values of ΔE, catechol presented the lowest reactivity. From an experimental point of view, the possible way of enhancing the adsorptive process and the sensitivity of the method is to use adequate substituents. This can change the stability of the complex, the net charge, and even the solubility of the ligand and complex as well. In our study, pyrogallol was more soluble in water than catechol due to the presence of three oxygen atoms and this was more useful for analytical purposes [60]. The electronegativity, χ has been proven to be a useful quantity in chemical reactivity theory. When two systems, in this case antimony and the two organic molecules, are joined, electrons will flow from the lower χ value to the higher χ value (Sb) until the equalization of chemical potentials. As shown in Table 1, catechol has a slightly larger χ value of 0.099 a.u. with respect to pyrogallol that has only 0.090 a.u.

Another important parameter is the electrophilicity index, ω which indicates the tendency of the molecule to accept electron (s). We have to notice here that the two studied molecules showed the electrophilicity values of 0.62 eV for catechol and 0.51 eV for pyrogallol. Thus, the unoccupied d-orbitals of the Sb atom could accept electrons from these molecules to form coordinate bonds. The studied molecules could accept electrons from the Sb atom with its anti-bonding orbitals to form back-donating bonds. These donation and back-donation processes strengthen the adsorption of the two ligands onto the metal surface, which is similar to previously drawn conclusions in the literature. The nucleophilicity values showed that pyrogallol was more reactive than catechol, which means high tendency of pyrogallol to bind with antimony surface and hence very strong metal-organic interaction.

116   Naceur Benhadria, Boulanouar   The Study of the Correlation between the Detection
         Messaoudi and Tarik Attar   Limit and the Energy Stability of Two Antimony
                                                 Complexes by Means of Conceptual DFT

Table 1. HOMO and LUMO energies, global reactivity indices μ, η, ω, and N, at B3LYP/6-31G* level of theory.

Substrate	HOMO (a.u.)	LUMO (a.u.)	μ (a.u.)	η (a.u.)	ω (eV)	N (eV)	Gap (a.u.)
Catechol	-0.206	0.008	-0.099	0.214	0.62	3.50	0.214
Pyrogallol	-0.200	0.019	-0.090	0.219	0.51	3.67	0.219

Table 2. Fukui (f^-) and DFT-based (N_k) indices of the selected atoms for catechol using NPA population analyses at B3LYP/6-31G* level of theory.

Atom k	f^+	f^-	N_k
C1	0.051	0.096	0.338
C2	0.048	0.155	0.541
C3	0.204	-0.001	-0.005
C4	0.067	0.107	0.376
C5	0.050	0.107	0.374
C6	0.203	0.025	0.088
O11	0.043	0.146	0.513
O13	0.036	0.094	0.329

Moreover, the Fukui (f^-) indices also showed that the molecules could be very reactive at O_{10} and O_{12} oxygen sites for pyrogallol and O_{11} and O_{13} oxygen sites for catechol. This reactivity was also related to the high nucleophilic character at these sites. The comparative study of the relative stabilities of the formed complexes. i.e., catechol and pyrogallol complexes (shown in Fig. 4), provided a clear idea about the relationship that could be established between the detection limit and the complex stability.
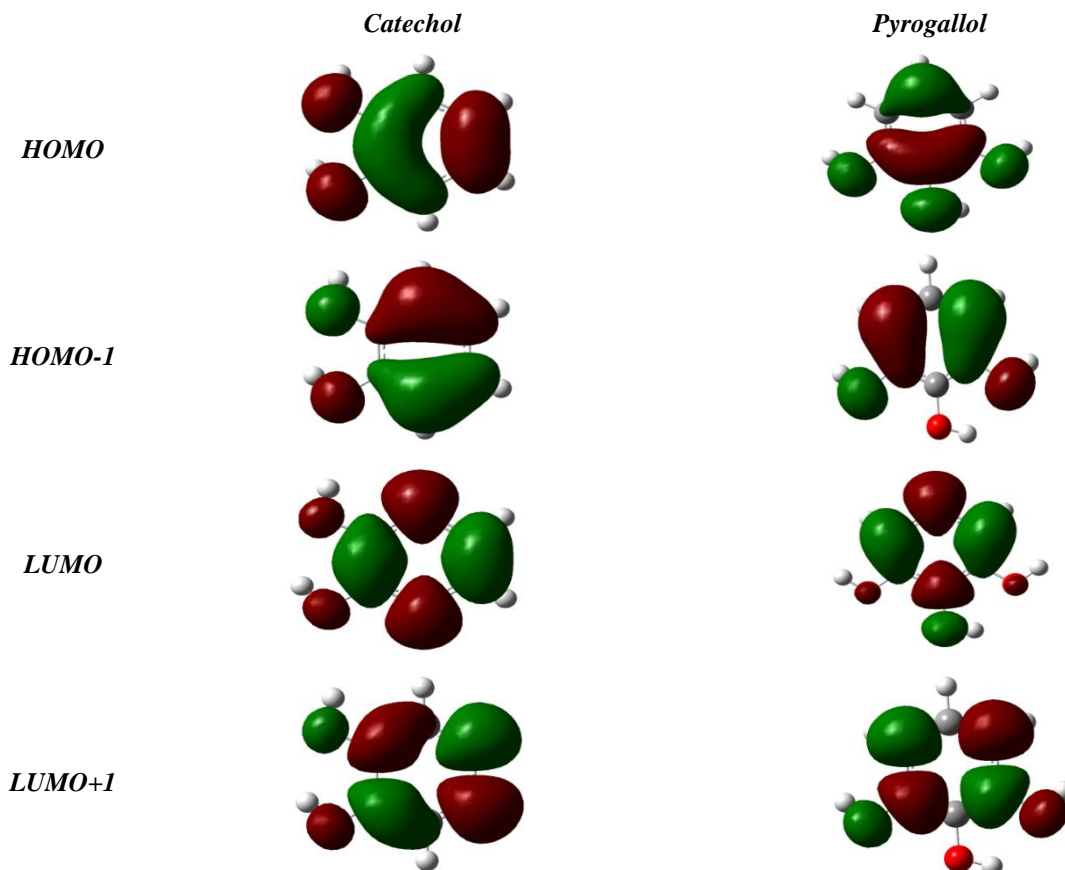

Figure 3. Calculated HOMO, HOMO-1, LUMO, and LUMO+1 molecular orbitals of the studied molecules at the LSDA/6-31G level of theory

117   Naceur Benhadria, Boulanouar
        Messaoudi and Tarik Attar

The Study of the Correlation between the Detection
Limit and the Energy Stability of Two Antimony
Complexes by Means of Conceptual DFT

Table 3. Fukui (f⁻) and DFT-based (N_k) indices of the selected atoms for the pyrogallol using NPA population analyses at B3LYP/6-31G* level of theory.

Atom k	f^+	f^-	N_k
C1	0.048	0.043	0.159
C2	0.222	0.147	0.541
C3	0.081	0.007	0.026
C4	0.026	0.068	0.252
C5	0.179	0.135	0.497
C6	0.049	0.042	0.157
O10	0.055	0.154	0.568
O12	0.036	0.091	0.337
O14	0.031	0.054	0.199
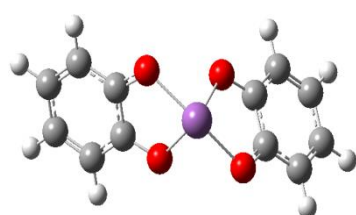
E = -7039.323 a.u
Catechol complex
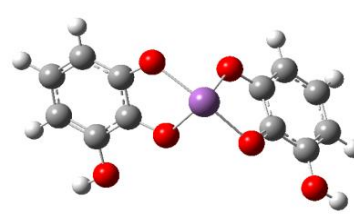
E = -7188.201 a.u
Pyrogallol complex

Figure 4. Molecular structures of the studied complexes at the LSDA/3-21G* level of theory.

The quantum chemical calculations using thermodynamical parameters such as Gibbs free energy have shown good correlations between the theoretical and experimental results. In a manner to confirm this tendency, a deep energetic comparison of the two molecules revealed that the antimony complexes were more stable energetically and thermodynamically with respect to their linked molecules (Table 4). From the energy values presented in Figure 4 above, we can see that the pyrogallol complex was more stable than the catechol complex with detection limits of 1.03×10^{-10} M and 1.3×10^{-9} M, respectively. Fundamentally, the stability of a metal complex can be explained with the help of thermodynamic stability. In other words, the thermodynamic stability of a metal complex is the measure of tendency of a metal ion to selectively form a specific metal complex and is directly related to the metal-ligand bond energy. So, the bond energy in the pyrogallol complex is greater than in the catechol complex. The stable complex has a high formation constant, which means that the metal is more dissimulated in the metal complex structure. In fact, a complex is any species involving coordination of ligands to a metal center. The metal center can be an atom or anion, and the complex can be a cation, an anion, or a neutral molecule. A common feature shared by the ligands in coordination complexes is the ability to donate electron pairs to central metal atoms or ions. Ligands are Lewis bases. In accepting electron pairs, central metal atoms or ions act as Lewis acids. Low energy of stability for the pyrogallol complex indicated that antimony ion has a greater affinity for pyrogallol (a stronger Lewis base) than catechol. So, we can say that the more stable is the complex, the better is its detection limit in AdSV technique.

Table 4. Values of energy, enthalpy, free energy, and entropy calculated in the gas phase at LSDA/3-21G* level of theory

	E (a.u.)	H (a.u.)	G (a.u.)	S (cal.K⁻¹.mol⁻¹)
Sb^{3+}	-6284.219	-6284.216	-6284.236	41.661
Catechol	-378.547	-378.432	-378.470	79.408
Pyrogallol	-452.988	-452.869	-452.909	85.472
Catechol complex	-7039.323	-7039.136	-7039.192	118.403
Pyrogallol complex	-7188.201	-7188.005	-7188.067	130.181

118 Naceur Benhadria, Boulanouar
Messaoudi and Tarik Attar

The Study of the Correlation between the Detection
Limit and the Energy Stability of Two Antimony
Complexes by Means of Conceptual DFT

CONCLUSIONS

In this paper, we have used the LSDA/B3LYP theoretical method in conjunction with 6-31G* and 3-21G* basis sets to investigate the complexation of two organic substances, pyrogallol and catechol, by antimony Sb(III). The study was conducted in order to probe the structural and electronic properties, on one hand to elucidate the reactivity and selectivity of the molecule centers, and on the other hand to find a relationship between the detection limit and the energetic stability of the formed complexes. We have found that the selective centers were only the neighbouring oxygens atoms (when bonding with antimony). The calculated energies showed that the complex formed with pyrogallol was more stable energetically and thermodynamically than the catechol complex which was in the same trend of their corresponding detection limits. Based on DFT calculations and the experimental results, the study has proved the possible existing link between the stability energy of the formed complexes and the detection limit. The study can give to the scientific researches a quantum novel way for the prediction of such phenomena and can be considered as a complementary tool to better understand the experimental results.

REFERENCES

1. Shotyk, W., Krachler, M., Chen, B. (2006) Contamination of Canadian and European bottled waters with antimony leaching from PET containers. *J. Environ. Monit.,* **8***,* 288–292.

2. Filella, M., Williams, P. A., Belzile, N. (2009) Antimony in the environment: knowns and unknowns. *Environ. Chem.,* **6**, 95–105.

3. Filella, M., Belzile, N., Chen, Y. W. (2002) Antimony in the environment: a review focused on natural waters. I. Occurrence. *Earth-Sci. Rev.,* **57**, 125–176.

4. Attar, T., Harek, Y., Larabi, L. (2012) Determination of copper levels in whole blood of healthy subjects by anodic stripping voltammetry. *Inter. Anal. Bioanal. Chem*., **2**, 160–164.

5. Attar T., Medjati, N., Harek, Y., Larabi, L. (2013) The Application of Differential Pulse Cathodic Stripping Voltammetry in the Determination of Trace Copper in Whole Blood. *J. Sens. Instrum.,* **1**, 31–38.

6. Attar T., Medjati N., Harek Y., Larabi L. (2013) Determination of Zinc levels in Healthy Adults from the West of Algeria by Differential Pulse Anodic Stripping Voltammetry. *JAC,* **6,** 855–860.

7. Attar, T., Harek, Y., Larabi, L. (2014) Determination of copper in whole blood by differential pulse adsorptive stripping voltammetry. *Mediterr. J. Chem.,* **2**, 691–700.

8. Abbasi, S., Khani, H., Tabaraki, R. (2010) Determination of ultra trace levels of copper in food samples by a highly sensitive adsorptive stripping voltammetric method. *Food Chem.,* **123**, 507–512.

9. Attar, T., Harek, Y., Larabi, L. (2013) Determination of Ultra Trace Levels of Copper in Whole Blood by Adsorptive Stripping Voltammetry. *J. Korean Chem. Soc.,* **57**, 568–573.

10. A. Percio, F. Mardini, A. C. Arnaldo, (2014) Determination of Xanthine in the Presence of Hypoxanthine by Adsorptive Stripping Voltammetry at the Mercury Film Electrode. *Anal. Chem. Insights.,* **9***,* 49–55.

11. Rojas, C., Arancibia, V., Gomez, M., Nagles, E. (2013) High sensitivity adsorptive stripping voltammetric method for antimony (III) determination in the presence of quercetin-5′-sulfonic acid. Substituent effect on sensitivity. *Sens. Actuator B-Chem.,* **185,** 560–567.

12. Rojas, C., Arancibia, V., Gomez, M., Nagles, E. (2013) Simultaneous determination of antimony (III) and molybdenum (VI) by adsorptive stripping voltammetry using quercetin as complexing agent. *Electroanalysis.,* **25**, 439–447.

13. Alghamdi, A. H. (2010) Determination of zinc by square-wave adsorptive stripping voltammetry using alizarin as a chelating agent. *J. Saudi. Chem. Soc.,* **14**, 1–7.

14. Edgar, N., Verónica, A., Roxana, R., Carlos, R. (2012) Simultaneous Determination of Lead and Cadmium in the Presence of Morin by Adsorptive Stripping Voltammetry with a Nafion–Ionic Liquid–coated Mercury Film Electrode. *Int. J. Electrochem. Sci.,* **7**, 5521–5533.

15. Elghalban, M. G., El Defarwy, A. M., Shah, R. K., Morsi, M. A. (2014) α-Furil Dioxime: DFT Exploration and its Experimental Application to the Determination of Palladium by Square Wave Voltammetry. *Int. J. Electrochem. Sci.,* **9**, 2379–2396.

16. Erden, S., Durmus, Z., Kilic, E. (2011) Simultaneous determination of antimony and lead in gunshot residue by cathodic adsorptive stripping voltammetric methods. *Electro-analysis.,* **23**, 1967–1974.

17. Jesus Gomez, G. M., Domınguez, R. O., Arcos-Martınez, M. J. (2007) Speciation of antimony by adsorptive stripping voltammetry using pyrogallol. *Talanta.,* **71**, 691–698.

119   Naceur Benhadria, Boulanouar
       Messaoudi and Tarik Attar

The Study of the Correlation between the Detection
Limit and the Energy Stability of Two Antimony
Complexes by Means of Conceptual DFT

18.   Yuki, F., Yuki, D., Shinji, K., Jun-ichiro, H., Koyo, N. (2017) Theoretical Study on the Kinetics of Thermal Decomposition of Guaiacol and Catechol. *J. Phys. Chem. A.*, **121**, 8495–8503.

19.   Güell, M., Siegbahn, P. (2007) Theoretical study of the catalytic mechanism of catechol oxidase. *J. Biol. Inorg. Chem.* **12**, 1251–1264.

20.   Catherine, B., Katalin, S., Stéphane, T., Jean-Louis, P. (2007) Chemical tools for mechanistic studies related to catechol oxidase activity. *C. R. Chim.*, **10**, 271–283.

21.   Krum, C., Joseph, J. B. (2006) Oxidation of catechol to muconic acid: A theoretical study, *J. Mol. Struct.,* **761**, 209–215.

22.   Mohammednoor, A., Bogdan, Z. D., Eric, M. K., John, C. M. (2010) Theoretical Study of Unimolecular Decomposition of Catechol. *J. Phys. Chem. A.,* **114**, 1060–1067.

23.   Zhang, H. Y., Sun, Y. M., Wang, X. L. (2003) Substituent effects on O-H bond dissociation enthalpies and ionization potentials of catechols: A DFT study and its implications in the rational design of phenolic antioxidants and elucidation of structure–activity relationships for flavonoid antioxidants. *Chem. Eur. J.*, **9**, 502–508.

24.   Vedernikova, I., Proynov, E., Salahub, D., Haemers, A. (2000) Local atomic and orbital reactivity indices from density functional calculations for hydrogen-bonded 1,2-dihydroxybenzene. *Int. J. Quantum. Chem.*, **77**, 161–173.

25.   Walther, C., Salvatore, D. B., Lothar, S., Susan, Q. K. N., Khamis, S. (1999) Investigation of the molecular structure of catechol by combined microwave spectroscopy and AB initio calculations. *J. Mol. Struct.,* **240**, 263–274.

26.   Daniel, F. S., Stephen, K. D., Paul, B. L., Chengchen, G., Gregory, P. H., Tijana, R., Kimberly, A. G., Jeffery, L. Y., Monica, C. (2016) Direct evidence of chelated geometry of catechol on TiO2 by a combined solid-state NMR and DFT study. ACS Publications. Journal contribution.

27.   Vedernikova, I., Salahub, D., Proynov, E. (2003) DFT study of hyperconjugation effects on the charge distribution in pyrogallol. *J. Mol. Struct.*, **663**, 59–71.

28.   Riahi, S., Moghaddam, A. B., Ganjali, M. R., Norouzi, P. (2007) Determination of the oxidation potentials of pyrogallol and some of its derivatives: theory and experiment. *J. Theoret. Comput. Chem.*, **6**, 331–340.

29.   Ji, H. F., Zhang, H. Y. (2005) A CCSD estimation of the O–H bond dissociation enthalpies of pyrogallol. *New. J. Chem.*, **29**, 535–537.

30.   Jiaqi, N., Lilin L., Yi, L., (2019) Antiradical and antioxidative activity of azocalix[4]arene derivatives: Combined experimental and theoretical study. *Molecules.*, **24**, 485–495.

31.   Siegel, S. M., Siegel, B. Z. (1958) Autoxidation of pyrogallol: General characteristics and inhibition by catalase. *Nature.*, **181**, 1153–1154.

32.   Li, X. (2012) Improved pyrogallol autoxidation method: A reliable and cheap superoxide-scavenging assay suitable for all antioxidants. *J. Agric. Food Chem.*, **60**, 6418–6424.

33.   Marklund, S., Marklund, G. (1974) Involvement of the superoxide anion radical in the autoxidation of pyrogallol and a convenient assay for superoxide dismutase. *Eur. J. Biochem.*, **47**, 469–474.

34.   Ardila, J. A., Oliveira, G. G., Medeiros, R. A. (2013) Determination of gemfibrozil in pharmaceutical and urine samples by square-wave adsorptive stripping voltammetry using a glassy carbon electrode modified with multi-walled carbon nanotubes within a dihexadecyl hydrogen phosphate film. *J. Electroanal. Chem.*, **690**, 32–37.

35.   Illuminati, S., Annibaldi, A., Truzzi, C. (2015) Determination of water-soluble, acid-extractable and inert fractions of Cd, Pb and Cu in Antarctic aerosol by square wave anodic stripping voltammetry after sequential extraction and microwave digestion. *J. Electroanal. Chem.*, **755**, 182–196.

36.   Frisch, M., Trucks, G., Schlegel, H., Scuseria, G. E., Robb, M. A., Cheeseman, J. R., (2009) Gaussian Inc Wallingford CT.

37.   Domingo, L., Aurell, M., Perez, P. (2002) Quantitative characterization of the global electrophilicity power of common diene/dienophile pairs in Diels-Alder reactions. *Tetrahedron.*, **58**, 4417–4423.

38.   Besler, B., Merz, K., Kollman, P. (1990) Atomic charges derived from semiempirical methods. *J. Comput. Chem.,* **11**, 431–439.

39.   Kurth, S., Perdew, J. P. (2000) Role of the Exchange–Correlation Energy: Nature's Glue. *Int. J. Quant. Chem.,* **5**, 814–818.

40.   Sen, K., Jorgenson, C. (1987) Springer Verlag, Berlin, Heidelberg, New York, London, Paris, Tokyo.

120 Naceur Benhadria, Boulanouar
Messaoudi and Tarik Attar

The Study of the Correlation between the Detection
Limit and the Energy Stability of Two Antimony
Complexes by Means of Conceptual DFT

41. Pal, S., Roy, R., Chandra, R. (1994) Change of Hardness and Chemical Potential in Chemical Binding: A Quantitative Model. *J. Phys. Chem. A.,* **98**, 2314–2317.

42. Geerlings, P., De Proft, F., Langenaeker, W. (2003) Conceptual Density Functional Theory. *Chem. Rev.,* **103**, 1793–1874.

43. Chermette, H. (1999) Chemical reactivity indexes in density functional theory. *J. Comput. Chem.,* **20**, 129–154

44. Pearson, R. G. (1999) Maximum Chemical and Physical Hardness. *J. Chem. Educ.,* **76**, 267–275.

45. Parr, R., von Szentpaly, L., Liu, S. (1999) Electrophilicity Index. *J. Am. Chem. Soc.,* **121**, 1922–1924.

46. Parr, R. G., Pearson, R. G. (1983) Absolute hardness: companion parameter to absolute electronegativity. *J. Am. Chem. Soc.,* **105**, 7512–7516.

47. Pearson, R. G. (1988) Absolute electronegativity and hardness: application to inorganic chemistry. *Inorg. Chem.,* **27**, 734–740.

48. Koopmans, T. (1933) Über die Zuordnung von Wellenfunktionen und Eigenwerten zu den Einzelnen Elektronen Eines Atoms. *Physica.,* **1**, 104–113.

49. Attar T., Messaoudi B., Benhadria, N. (2020) DFT Theoretical Study of Some Thiosemicarbazide Derivatives with Copper. *Chem. Chem. Technol.*, 2020, **14**, 20–25.

50. Jaramillo, P., Domingo, L., Chamorro, E. (2008) A further exploration of a nucleophilicity index based on the gas-phase ionization potentials. *J. Mol. Struct. Theochem.,* **865***,* 68–72.

51. Contreras, R., Andres, J., Safont, V. S., Campodonico, P., Santos, J. G. (2003) A Theoretical Study on the Relationship between Nucleophilicity and Ionization Potentials in Solution Phase. *J. Phys. Chem. A.,* **107**, 5588–5593.

52. Abreu-Quijano, M., Palomar-Pardavé, M., Cuan, A., Romero-Romo, M., Negrón-Silva, G. (2011) Quantum Chemical Study of 2-Mercaptoimidazole, 2-Mercaptobenzimidazole, 2-Mercapto-5-Methylbenzimidazole and 2-Mercapto-5-Nitrobenzimidazole as Corrosion Inhibitors for Steel. *Int. J. Electrochem. Sci.,* **6**, 3729–3742.

53. Haghdadi, M. Amani, H. Nab, N. (2015) Theoretical study on the Diels–Alder reaction of bromo-substituted 2H-pyran-2-ones and some substituent vinyls. *J. Serb. Chem. Soc.,* **80**, 1139–1148.

54. Parr, R., Yang, W. (1984) Density functional approach to the frontier-electron theory of chemical reactivity. *J. Am. Chem. Soc.,* **106**, 4049–4050.

55. Yang, W., Mortier, W. (1986) The use of global and local molecular parameters for the analysis of the gas-phase basicity of amines. *J. Am. Chem. Soc.,* **108**, 5708–5711.

56. De Proft, F., Martin, J., Geerlings, P. (1996) Calculation of molecular electrostatic potentials and Fukui functions using density functional methods. *Chem. Phy. Lett.,* **256**, 400–408.

57. Nguyen, L., Ngoc, L., De Proft, F. (1999) Mechanism of [2 + 1] Cycloadditions of Hydrogen Isocyanide to Alkynes: Molecular Orbital and Density Functional Theory Study. *J. Am. Chem. Soc.,* **121**, 5992–6001.

58. Alam, M. J., Shabbir, A. (2012) Anharmonic vibrational studies of l-aspartic acid using HF and DFT calculations. *Spectrochim. Acta. A. Mol. Biomol. Spectrosc.*, **96**, 992–1004.

59. Demir, P., Akman, F. (2017) Molecular structure, spectroscopic characterization, HOMO and LUMO analysis of PU and PCL grafted onto PEMA-co-PHEMA with DFT quantum chemical calculations. *J. Mol. Struct.*, **1134**, 404–415.

60. Kopacz, M. (2003) Quercetin- and morinsulfonates as analytical reagents. *J. Anal. Chem.*, **58**, 225–229.